

Electron Turbulence at Nanoscale Junctions

Neil Bushong,^{*,†} John Gamble,[‡] and Massimiliano Di Ventra[†]

*Department of Physics, University of California, San Diego,
La Jolla, California 92093-0319, and Department of Physics, The College of Wooster,
Wooster, Ohio 44691-2363*

Received April 20, 2007; Revised Manuscript Received May 7, 2007

ABSTRACT

Electron transport through a nanostructure can be characterized in part using concepts from classical fluid dynamics. It is thus natural to ask how far the analogy can be taken and whether the electron liquid can exhibit nonlinear dynamical effects such as turbulence. Here we present an ab initio study of the electron dynamics in nanojunctions which reveals that the latter indeed exhibits behavior quite similar to that of a classical fluid. In particular, we find that a transition from laminar to turbulent flow occurs with increasing current, corresponding to increasing Reynolds numbers. These results reveal unexpected features of electron dynamics and shed new light on our understanding of transport properties of nanoscale systems.

Electron transport through a nanoscale junction is usually described as a scattering problem.^{1–9} On the other hand, it has been shown^{10–13} that the behavior of the electron liquid obeys dynamical equations of motion which are similar in form to those governing the dynamics of classical liquids. In particular, it was recently shown¹³ that the time-dependent Schrödinger equation (TDSE) for electrons flowing across a nanostructure can be cast in the form of generalized Navier–Stokes equations. A consequence of this analogy is the prediction that under certain conditions the laminar flow of the liquid may become unstable and turbulent behavior is expected.^{13–15} One can then borrow knowledge from classical fluid dynamics and hypothesize that the electron flow will make a transition from laminar to turbulent regimes, if, e.g., the current is increased. As in a classical liquid, if, for instance, electrons flow from one electrode (call it the top electrode) to another (call it the bottom electrode) across a nanojunction, turbulence would first manifest itself with the break-up of the top-down symmetry of the electron flow.^{14,15} By increasing the current further, one should observe the formation of eddies in proximity to the junction. These turbulent eddies are created because of the larger kinetic energy in the direction of current flow (longitudinal kinetic energy) compared to the transverse direction (transverse kinetic energy). With further increase of the current, the disparity between longitudinal and transverse components of the kinetic energy increases, and the system flow eventually breaks any remaining symmetry, thus developing turbulence fully.^{14,15} Despite the prediction of turbulent

behavior of the electron liquid in nanostructures¹³ an explicit demonstration of this phenomenon and the analysis of its microscopic features have not been presented yet.

In this paper we show numerically turbulent effects for the electron liquid crossing a nanojunction both by solving directly the TDSE and by solving the generalized Navier–Stokes equations derived in ref 13. These read

$$D_t n(\mathbf{r}, t) = -n(\mathbf{r}, t) \nabla \cdot \mathbf{u}(\mathbf{r}, t)$$

$$mn(\mathbf{r}, t) D_t u_i(\mathbf{r}, t) = -\partial_i P(\mathbf{r}, t) + \partial_j \pi_{ij} - n(\mathbf{r}, t) \partial_i V_{\text{ext}}(\mathbf{r}, t) \quad (1)$$

Here, n is the electron density, $\mathbf{u} = \mathbf{j}/n$ is the velocity field, i.e., the ratio between the current density \mathbf{j} and the density, and $D_t = (\partial/\partial t) + \mathbf{u} \cdot \nabla$ is the convective derivative.¹⁵ $P(\mathbf{r}, t)$ is the pressure of the liquid, $V_{\text{ext}}(\mathbf{r}, t)$ an external potential, and π_{ij} is a traceless tensor that describes the shear effect on the liquid. It has the form

$$\pi_{ij} = \eta \left(\partial_i u_j + \partial_j u_i - \frac{2}{3} \delta_{ij} \partial_k u_k \right) \quad (2)$$

where $\eta = \hbar n f(n)$ is the viscosity of the electron liquid and $f(n)$ is a smooth function of the density.¹⁶

In analogy with the classical case we expect that the atomic structure, and in particular atomic defects in proximity to the junction, play the role of “obstacles” for the liquid and thus favor turbulence. Since we aim at showing that turbulence develops irrespective of the underlying atomic structure, we consider electrons interacting with a uniform positive background charge (i.e., the “jellium” model¹⁷). The

* Corresponding author: bushong@physics.ucsd.edu.

[†] University of California.

[‡] The College of Wooster.

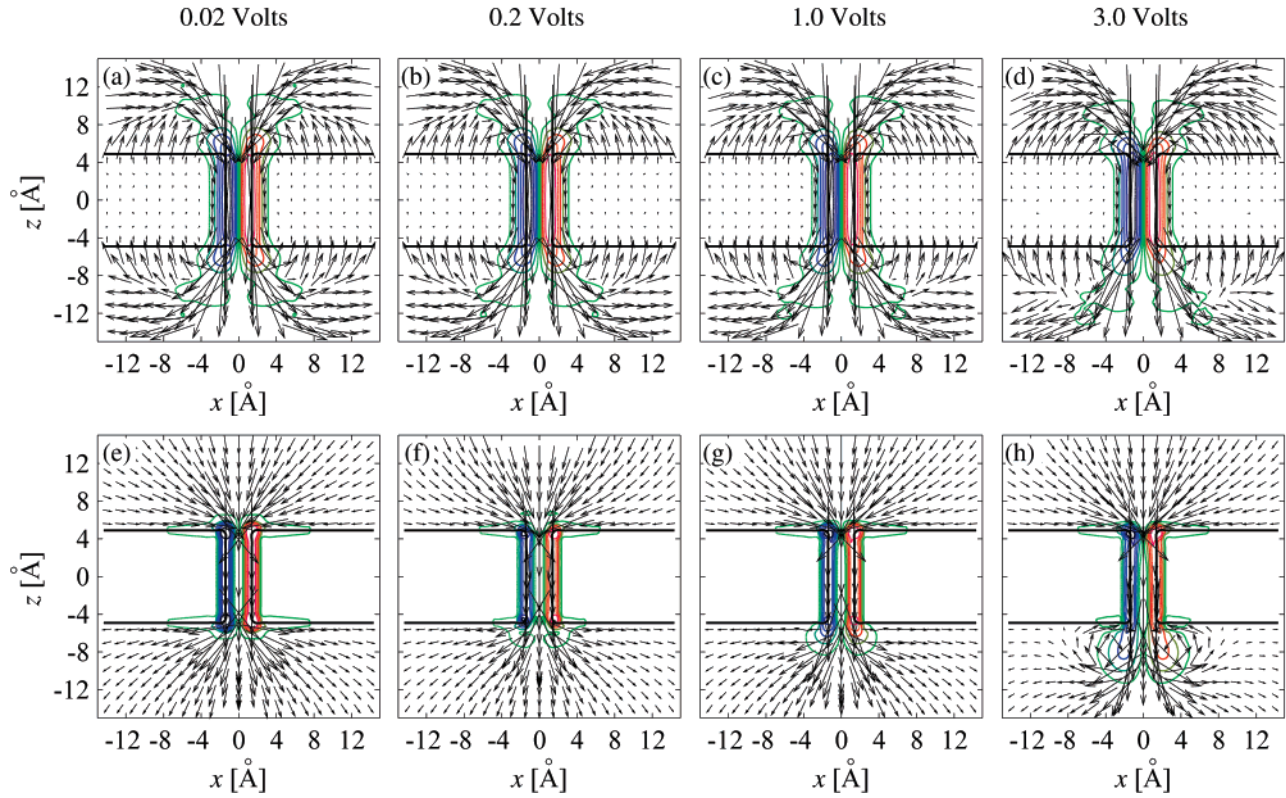


Figure 1. (a–d) Electron current density for electrons moving from the top electrode to the bottom electrode across a nanojunction at $t = 1.4$ fs, for an initial bias of (a) 0.02, (b) 0.2, (c) 1.0, and (d) 3.0 V. The arrows denote the current density, while the level sets denote the curl of the 2D current density. The solid lines delimit the contour of the junction. (e–h) Velocity field solution of the eqs 1, for a liquid with same velocity, density, and viscosity as the quantum mechanical one.

system we consider therefore consists of two large but finite jellium electrodes—subject to a bias—connected via a nano-scale jellium bridge. (The jellium edge of this system is represented with solid lines in each panel of Figure 1.) We choose the density of the jellium at equilibrium typical of bulk gold ($r_s \approx 3a_0$). For computational convenience we choose a quasi-two-dimensional (quasi-2D) system, approximately 2.8 \AA thick.³⁵ Note that, everything else being equal, a quasi-2D geometry disfavors turbulence compared to a 3D one. We thus expect that if turbulence develops in our chosen quasi-2D geometry with given thickness, then turbulence will develop even more easily if we leave everything else unchanged (including the total current) and increase the thickness of the electrodes.

The solution of the TDSE for the many-body system is obtained within time-dependent current density functional theory (TDCDFT);¹¹ i.e., for each single-particle state ϕ_α , we have solved the equation of motion (in atomic units)

$$\left\{ i \frac{\partial}{\partial t} - \frac{1}{2} \left(\frac{1}{i} \nabla - \frac{1}{c} \mathbf{a}_{xc} \right)^2 - v_{jel} - v_H - v_{xc} \right\} \phi_\alpha = 0 \quad (3)$$

where c is the speed of light, v_{jel} is the potential due to the jellium, v_H is the Hartree potential, and v_{xc} is the exchange-correlation scalar potential.³⁶ The shear viscosity of the electron liquid η enters the problem through the exchange-correlation vector potential \mathbf{a}_{xc} .^{11,16} If we make the approximation that, at any given time, the viscosity is a function of

the density only, and does not depend on time explicitly, we find that the i th component of \mathbf{a}_{xc} evolves according to¹⁶

$$\frac{1}{c} \frac{\partial a_{xc,i}}{\partial t} = \frac{1}{n} \sum_j \left\{ \eta \frac{\partial^2 u_i}{\partial r_j^2} + \frac{\eta}{3} \frac{\partial^2 v_j}{\partial r_i \partial r_j} + \frac{\partial \eta}{\partial r_j} \left(\frac{\partial u_i}{\partial r_j} + \frac{\partial u_j}{\partial r_i} \right) - \frac{2}{3} \frac{\partial \eta}{\partial r_i} \frac{\partial u_j}{\partial r_j} \right\} \quad (4)$$

For the viscosity η of the electron liquid we have used the one reported in ref 16. We employ the approach described in refs 18–21 to initiate electron dynamics and calculate the current. We prepare the system by placing it in its ground state; because of the applied bias, the system exhibits a separation of charge. At a time $t = 0$, we remove the bias and let the system evolve according to eq 3.³⁷ After long time scales, the electrons encounter the far boundaries of the jellium electrodes and reflect. However, we are interested in comparing the electron dynamics calculated from eq 3 with the one obtained by solving the Navier–Stokes equation (eq 1), at times smaller than this reflection time. Equation 1 is solved by assuming the same density, initial velocity, and viscosity of the liquid employed in the TDCDFT calculation.³⁸ We also solve eq 1 by assuming the liquid to be incompressible. This simplifies the calculations enormously but leads to some differences with the solutions of eq 3 (see discussion later).

Figure 1 depicts the flow of electrons across the nanostructure, for a range of biases between 0.02 and 3.0 V, after the initial transient. Panels a–d correspond to the solution of the TDSE (eq 3); panels e–h to the solution of the Navier–Stokes equation (eqs 1) using the same set of parameters.²² Panel a has to be compared with panel e; panel b with f, and so on. As anticipated, we observe some differences between the solutions of the eq 1 and the solutions of eq 3. These differences are due to the details of the charge configuration at the electrode–junction interface, and some degree of compressibility of the quantum liquid in the junction.³⁹

From Figure 1 we can see the effect of surface charges, in that some electrons flow parallel to the surfaces.²⁰ More importantly, at low biases, the flow is laminar and “smooth”. In addition, at these biases the current density shows an almost perfect top–bottom symmetry: the direction of the flow is symmetric with respect to the operation $z \rightarrow -z$. This symmetry is even more evident by comparing the curl of the current density in the top and bottom electrodes (see for instance parts a and e of Figure 1).

With increase of the bias, however, a transition occurs: the symmetry $z \rightarrow -z$ of the current density breaks completely, and eddies start to appear in proximity to the junction. This is clearly evident, for instance, in parts d and h of Figure 1. The outgoing current density in the bottom electrode has a more varied angular behavior, in contrast to the behavior in the top electrode, in which the electron liquid flows more uniformly toward the junction.

Since the panels e–h of Figure 1 practically describe the dynamics of a classical fluid with the same parameters as the quantum liquid, the analogy between the electron flow and the one of a classical liquid is quite evident. We can push this analogy even further by defining a Reynolds number for the quantum system as well: $R = u_z L \rho / \eta$, where u_z is the longitudinal velocity in the junction, L is the width of the junction, and ρ is the density. Using the density of valence electrons in gold, and using the current density in the junction at $t = 1.4$ fs, we obtain for the quantum case the following Reynolds numbers: 0.216, 2.16, 10.8, and 32.5 for 0.02, 0.2, 1.0, and 3.0 V, respectively.

Just as in the classical case, we can then reinterpret the above results as follows. At low Reynolds numbers, the flow is highly symmetric from top to bottom. This symmetry is lost as the Reynolds number is increased. At high Reynolds numbers, the incident flow is laminar, while the outgoing flow has a jetlike character and “turns back” on itself creating local eddies in the current density. We stress here that while the TDCDFT current density does differ, in some details, from the one obtained from the Navier–Stokes equations, turbulent behavior (i.e., asymmetry and dynamical eddy-like formation) is observed in the fully quantum-mechanical calculation as well. The exact details of this turbulent behavior are dynamical in nature and cannot be captured by a static calculation.

Having shown the similarity between the current flow obtained using the Navier–Stokes equation (eq 1) and the one obtained solving the TDSE (3), we can study the first one at time scales prohibitive for full quantum mechanical simulations. We can also study the effect of a larger thickness

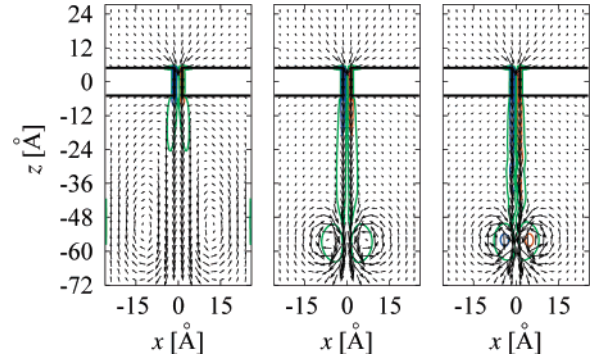


Figure 2. Current density (arrows) and curl of the current density (denoted by level sets) of the electron liquid, for three different Reynolds numbers, 32.5 (left panel), 162 (middle panel), and 325 (right panel). Note that the fluid velocity has lost perfect left–right symmetry in the middle- and right-panel cases.

of the electrodes on the turbulent flow by realizing that this is equivalent to increasing the Reynolds number (which, incidentally, is also equivalent to increasing the bias). This is illustrated in Figure 2 where the current density and the curl of the current density are plotted for the Reynolds number 32.5 of Figure 1h (left panel of Figure 2) and in the same system but with a Reynolds number five times larger (middle panel of Figure 2) and (right panel of Figure 2) with a Reynolds number ten times larger.

From Figure 2 it is evident that by increasing thickness the last remaining symmetry $x \rightarrow -x$ is broken at earlier times and closer to the junction. For instance, in the case represented in Figure 2 (middle panel), the left–right symmetry is lost at about 14 fs, with consequent asymmetric flow within about 50 Å from the junction center. For the structure represented in Figure 2 (right panel), the symmetry is broken at about 6 fs, and the flow asymmetry appears at about 25 Å from the junction.

We can better quantify the amount of turbulence by calculating the velocity correlation tensor¹⁵

$$B_{ik} = \langle (v_i(\mathbf{r}) - v_i(\mathbf{r} + \delta\mathbf{r}))(v_k(\mathbf{r}) - v_k(\mathbf{r} + \delta\mathbf{r})) \rangle \quad (5)$$

where $\delta\mathbf{r}$ is a given distance, and $i, k = x, y, z$. Here, the angle brackets $\langle \dots \rangle$ denote averaging over all positions \mathbf{r} within a given region. Fully developed and isotropic turbulence has a velocity correlation tensor that is a function only of the magnitude of $\delta\mathbf{r}$ and increases quadratically with distance.¹⁵ Instead, the turbulence in the examples of Figure 2 is not fully developed. The velocity correlation tensor, B_{ik} , thus depends on both the magnitude of $\delta\mathbf{r}$ and its direction. This is illustrated in Figure 3 where various components of B_{ik} are plotted at $t = 75.0$ fs for the system with Reynolds number 32.5 as a function of the magnitude of $\delta\mathbf{r}$, where we have chosen $\delta\mathbf{r}$ to point in the longitudinal (z) direction. The spatial averaging has been carried out over the left-hand side of the outgoing region (that is, in the region $z = [-27.3 \text{ Å}, -72.1 \text{ Å}]$, $x = [-25.9 \text{ Å}, 0.0 \text{ Å}]$, where the origin is in the center of the junction). For comparison, the same quantity is plotted for the laminar case, i.e., for a Reynolds number of 0.216. (To compare the laminar and turbulent cases, we have scaled the average turbulent velocity to the average

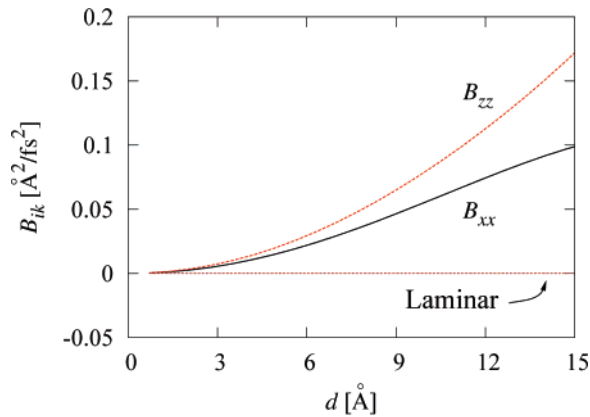


Figure 3. Various components of the velocity correlation tensor B_{ik} as a function of distance $d = |\delta \mathbf{r}|$, for a Reynolds number of $R = 32.5$. For the case where $R = 0.216$, the elements of B_{ik} are orders of magnitude smaller, and so the corresponding curves for the laminar case coincide with the x axis.

laminar velocity.) As expected, in the laminar case the correlation tensor is essentially zero, while for the turbulent case it increases with distance.

We conclude by noting that an experiment in which the electron flow can be monitored directly may measure nonlaminar electron behavior as an asymmetry between the incoming and outgoing patterns of the current density through a nanojunction. Experiments similar to the ones reported in ref 23, which use scanning probe microscopy to image the flowlines, may provide such capabilities. Note, however, that since these scanning probe techniques record images over time scales much longer than the turbulent electron dynamics, one would expect that in the turbulent regime images of current flow appear “smeared out” compared to the laminar case and asymmetric in the incoming and outgoing patterns. One can also envision the possibility of using the magnetic field produced by the current to probe the electrons’ transition to turbulence: the magnetic field on the top electrode would be different from the magnetic field in the bottom electrode (turbulent region). We will explore this possibility in an upcoming work.²⁴ From the present work and the analytical results obtained in ref 13, we also suggest that fully 3D and nonadiabatic junctions, i.e., junctions with a geometry that changes abruptly (like the one explored in this work), are the best candidates to observe turbulence. We also expect defects and other impurities to favor turbulent behavior by playing the role of “obstacles” for the electron flow.

We finally note that turbulent behavior may have consequences on the formation (or lack thereof) of local equilibrium distributions in the electrodes¹⁹ and may generate nontrivial local electron heating effects in the junction²⁵ and at the eddies sites; phenomena and properties which are still poorly understood at the nanoscale and ultimately may have unexpected consequences on the stability of nanostructures under current flow.^{26–28}

Acknowledgment. We acknowledge useful discussions with Roberto D’Agosta. J.G. received support from the National Science Foundation’s REU program. This work was supported by the U.S. Department of Energy under Grant DE-FG02-05ER46204.

References

- (1) Landauer, R. *IBM J. Res. Dev.* **1957**, *1*, 223.
- (2) Büttiker, M.; Imry, Y.; Landauer, R.; Pinhas, S. *Phys. Rev. B* **1985**, *31*, 6207.
- (3) Di Ventra, M.; Pantelides, S. T.; Lang, N. D. *Phys. Rev. Lett.* **2000**, *84*, 979. Di Ventra, M.; Pantelides, S. T.; Lang, N. D. *Phys. Rev. Lett.* **2001**, *86*, 288. Di Ventra, M.; Pantelides, S. T.; Lang, N. D. *Appl. Phys. Lett.* **2000**, *76*, 3448.
- (4) Emberly, E.; Kirczenow, G. *Phys. Rev. B* **1998**, *58*, 10911.
- (5) Prociuk, A.; Van Kuiken, B.; Dunietz, B. D. *J. Chem. Phys.* **2006**, *125*, 204717.
- (6) Taylor, J.; Guo, H.; Wang, J. *Phys. Rev. B* **2001**, *63*, 245407.
- (7) Damle, P. S.; Ghosh, A. W.; Datta, S. *Phys. Rev. B* **2001**, *64*, 201403(R).
- (8) Xue, Y.; Datta, S.; Ratner, M. A. *J. Chem. Phys.* **2001**, *115*, 4292.
- (9) Palacios, J. J.; Pérez-Jiménez, A. J.; Louis, E.; San-Fabián, E.; Vergés, J. A. *Phys. Rev. B* **2002**, *66*, 035322.
- (10) Martin, P. C.; Schwinger, J. *Phys. Rev.* **1959**, *115*, 1342.
- (11) Vignale, G.; Ullrich, C. A.; Conti, S. *Phys. Rev. Lett.* **1997**, *79*, 4878.
- (12) Tokatly, I. V. *Phys. Rev. B* **2005**, *71*, 165104.
- (13) D’Agosta, R.; Di Ventra, M. *J. Phys.: Condens. Matter* **2006**, *18*, 11059.
- (14) Frisch, U. *Turbulence*; Cambridge University Press: Cambridge, 1995.
- (15) Landau, L. D.; Lifshitz, E. M. *Fluid Mechanics*, 2nd ed.; Pergamon Press: New York, 1987; Vol. 6.
- (16) Conti, S.; Vignale, G. *Phys. Rev. B* **1999**, *60*, 7966.
- (17) Di Ventra, M.; Lang, N. D. *Phys. Rev. B* **2002**, *65*, 045402.
- (18) Di Ventra, M.; Todorov, T. N. *J. Phys.: Condens. Matter* **2004**, *16*, 8025.
- (19) Bushong, N.; Sai, N.; Di Ventra, M. *Nano Lett.* **2005**, *5*, 2569.
- (20) Sai, N.; Bushong, N.; Hatcher, R.; Di Ventra, M. *Phys. Rev. B* **2007**, *75*, 115410.
- (21) Cheng, C.-L.; Evans, J. S.; Voorhis, T. V. *Phys. Rev. B* **2006**, *74*, 155112.
- (22) Popinet, S. *J. Comput. Phys.* **2003**, *190*, 572.
- (23) Topinka, M. A.; LeRoy, B. J.; Shaw, S. E. J.; Heller, E. J.; Westervelt, R. M.; Maranowski, K. D.; Gossard, A. C. *Science* **2000**, *289*, 2323.
- (24) Bushong, N.; Pershin, Y.; Di Ventra, M. In preparation.
- (25) D’Agosta, R.; Sai, N.; Di Ventra, M. *Nano Lett.* **2006**, *6*, 2935.
- (26) Huang, Z. F.; Xu, B. Q.; Chen, Y.-C.; Di Ventra, M.; Tao, N. J. *Nano Lett.* **2006**, *6*, 1240.
- (27) Tsutsui, M.; Kurokawa, S.; Sakai, A. *Nanotechnology* **2006**, *17*, 5334.
- (28) Smit, R. H. M.; Untiedt, C.; van Ruitenbeek, J. M. *Nanotechnology* **2004**, *15*, S472.
- (29) Kohn, W.; Sham, L. *Phys. Rev.* **1965**, *140*, A1133.
- (30) Zangwill, A.; Soven, P. *Phys. Rev. Lett.* **1980**, *45*, 204.
- (31) Runge, E.; Gross, E. K. U. *Phys. Rev. Lett.* **1984**, *52*, 997.
- (32) Ceperley, D. M.; Alder, B. J. *Phys. Rev. Lett.* **1980**, *45*, 566.
- (33) Perdew, J. P.; Zunger, A. *Phys. Rev. B* **1981**, *23*, 5048.
- (34) Tal-Ezer, H.; Kosloff, R. *J. Chem. Phys.* **1984**, *81*, 3967.
- (35) Each electrode is 51.8 Å wide in the x direction, and 22.4 Å long in the z direction of current flow (see Figure 1). The width of the rectangular bridge is 2.8 Å, and the gap between the electrodes is 9.8 Å.
- (36) We have used the adiabatic local density approximation to the scalar exchange-correlation potential,^{29–31} as derived by Ceperley and Alder³² and parametrized by Perdew and Zunger.³³
- (37) The grid spacing of the jellium system is 0.7 Å, and the timestep used to propagate the system is 2.5×10^{-3} fs. We used the Chebyshev method³⁴ for constructing the time-evolution operator.
- (38) For the simulation of the Navier–Stokes equations, we use Dirichlet boundary conditions for the velocity at the inlet, and Neumann boundary conditions at the outlet.
- (39) The issue of compressibility is also related to the treatment of the fluid at the boundaries of the confining structure. In general, wavefunctions tend to exhibit exponentially decreasing density at the edges of a confining potential, while incompressible classical fluids are described with hard walls and “no-slip” boundary conditions. The assumption in the Navier–Stokes equations that the electron liquid is incompressible also neglects the formation of surface charges; for a discussion of dynamical charging effects near nanoscopic junctions, see ref 20.

NL070935E